Developmental Cell
Article

The Molecular Basis of Vascular Lumen Formation in the Developing Mouse Aorta

Boris Strilić,[1,2] Tomáš Kučera,[2,3] Jan Eglinger,[1,2] Michael R. Hughes,[4] Kelly M. McNagny,[4] Sachiko Tsukita,[5] Elisabetta Dejana,[6] Napoleone Ferrara,[7] and Eckhard Lammert[1,2,*]
[1]Institute of Metabolic Physiology, Heinrich-Heine-University of Düsseldorf, 40225 Düsseldorf, Germany
[2]Max Planck Institute of Molecular Cell Biology and Genetics, 01307 Dresden, Germany
[3]Institute of Histology and Embryology, First Faculty of Medicine, Charles University, 12800 Prague, Czech Republic
[4]University of British Columbia, Biomedical Research Centre, Vancouver, BC V6T 1Z3, Canada
[5]Osaka University, Laboratory of Biological Science, 565-0871 Osaka, Japan
[6]IFOM, FIRC Institute of Molecular Oncology, 20139 Milan, Italy
[7]Genentech Inc., South San Francisco, CA 94080, USA
*Correspondence: lammert@uni-duesseldorf.de
DOI 10.1016/j.devcel.2009.08.011

SUMMARY

In vertebrates, endothelial cells (ECs) form blood vessels in every tissue. Here, we investigated vascular lumen formation in the developing aorta, the first and largest arterial blood vessel in all vertebrates. Comprehensive imaging, pharmacological manipulation, and genetic approaches reveal that, in mouse embryos, the aortic lumen develops extracellularly between adjacent ECs. We show that ECs adhere to each other, and that CD34-sialomucins, Moesin, F-actin, and non-muscle Myosin II localize at the endothelial cell-cell contact to define the luminal cell surface. Resultant changes in EC shape lead to lumen formation. Importantly, VE-Cadherin and VEGF-A act at different steps. VE-Cadherin is required for localizing CD34-sialomucins to the endothelial cell-cell contact, a prerequisite to Moesin and F-actin recruitment. In contrast, VEGF-A is required for F-actin-nm-Myosin II interactions and EC shape change. Based on these data, we propose a molecular mechanism of in vivo vascular lumen formation in developing blood vessels.

INTRODUCTION

Blood vessels are multicellular tubes, essential for the transport of fluids, gases, and nutrients in all vertebrates. They are composed of endothelial cells (ECs) that form an interface between the circulating blood and the surrounding tissues. During blood vessel formation, ECs first assemble into multicellular cords before forming a vascular lumen (Czirok et al., 2008; Kamei et al., 2006). Previous findings suggest that, following cord formation, ECs form a lumen via coalescence of intracellular vacuoles that persist in ECs for several hours (Davis and Camarillo, 1996; Folkman and Haudenschild, 1980; Kamei et al., 2006; Sabin, 1920). Based on this model, large intracellular vacuoles give rise to so-called seamless blood vessels, which have no junctions in transverse section (Kamei et al., 2006). However, most blood vessels are not seamless, as they display auto- and intercellular junctions in transverse sections, indicating an alternative mechanism of vascular lumen formation (Blum et al., 2008; Drake and Fleming, 2000; Jin et al., 2005; Parker et al., 2004).

Here, we investigate vascular lumen formation in the developing aorta, which is the first and largest arterial blood vessel in all mammals (Drake and Fleming, 2000; Sato et al., 2008). In mice, similar to humans, the aorta develops from two lateral EC cords, called dorsal aortae, that fuse at later stages of development (Drake and Fleming, 2000; Lammert et al., 2001). Here, we show that lumen formation in the dorsal aortae within the developing mouse embryo is a temporally and spatially defined process. Analyzing the transition from an EC cord to a vascular tube via electron microscopy (EM) and confocal light microscopy, as well as via various pharmacological and genetic manipulation experiments, allowed us to propose a molecular mechanism of how the aortic lumen develops in vivo.

RESULTS

Aortic Lumen Formation Initiates between the 1S and 3S Stages of Mouse Embryonic Development

To determine the timing and positioning of the transition from an EC cord to a vascular tube, we used single-plane illumination microscopy (SPIM) and confocal light microscopy to image the developing dorsal aortae in whole mouse embryos and in transverse sections, respectively (Figure 1). At the 1–2 somite (1–2S) stage of mouse development, on embryonic day (E) 8.0 (Figure 1A), ECs formed clusters (Figures 1B and 1C; see Movie S1 available online). A few hours later, at the 3–5S stage (Figure 1D), continuous EC cords were observed (Figure 1E and Movie S1), most of which had formed a vascular lumen (asterisk in Figure 1F). By the 6–8S stage on E8.25 (Figure 1G), the dorsal aortae were enlarged (Figure 1H and Movie S1), and the process of lumen formation was complete (Figure 1I). During the next day of mouse development (Figure 1J), a complex circulatory system developed (Figure 1K and Movie S1), and the aortic lumen further increased (Figure 1L).

We conclude that lumen formation in the developing dorsal aortae initiates between the 1S and 3S stages of mouse embryonic development, followed by completion and expansion of the aortic lumen as well as vascular sprouting.

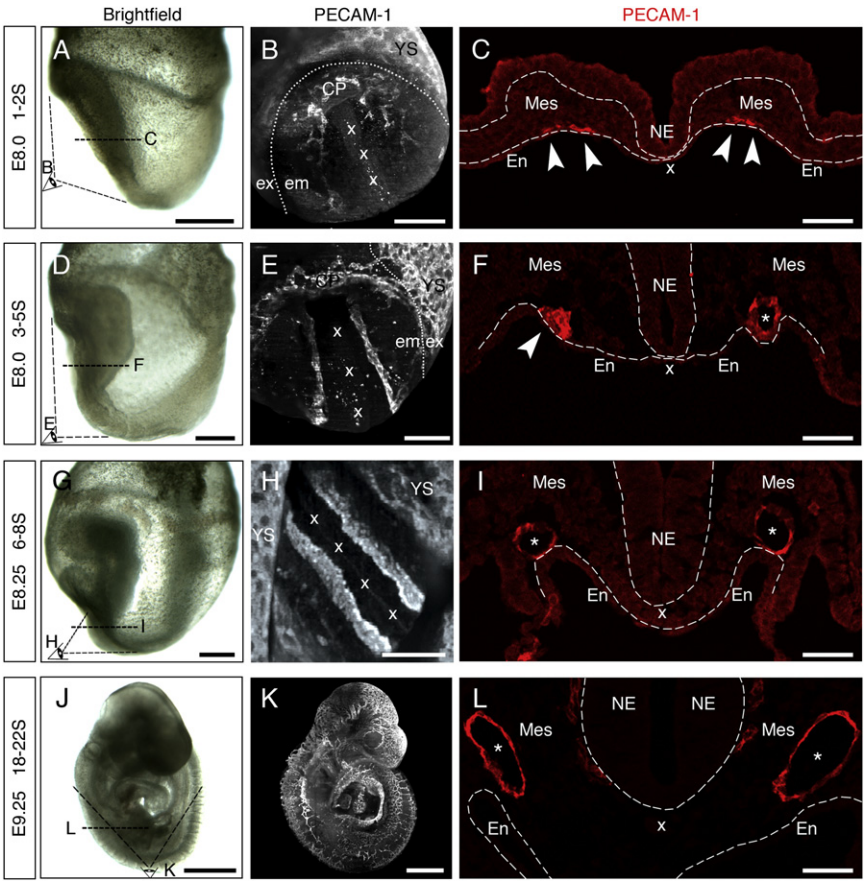

Figure 1. Lumen Formation in the Developing Aorta Is Initiated Between the 1S and 3S Stages of Mouse Development

(A, D, G, J) Lateral bright-field images of mouse embryos at the indicated embryonic stages (E8.0–E9.25; 1–22S stages).

(B, E, H, K) Three-dimensional, single-plane illumination microscopy (SPIM) images of mouse embryos at the indicated stages, stained for EC marker PECAM-1, and viewed as indicated in (A, D, G, J). CP, cardiogenic plate; em, embryonic tissue; ex, extraembryonic tissue; x, notochord; YS, yolk sac. See Movie S1.

(C, F, I, L) Confocal light microscopic images of transverse sections indicated in (A), (D), (G), and (J) through the ventral part of staged mouse embryos stained for PECAM-1. En, endoderm; Mes, mesenchyme; NE, neuroepithelium; x, notochord. Endothelial cell (EC) cords are indicated with arrowheads; aortic lumens are labeled with asterisks. Scale bars, 250 μm (A, B, D, E, G, H), 50 μm (C, F, I, L), and 500 μm (J, K).

The Aortic Lumen Develops Extracellularly

To investigate the onset of vascular lumen formation, we performed an ultrastructural EM analysis of transverse sections through the developing dorsal aortae. At the 1S stage (Figure 2A), ECs clustered and were connected by junctions at multiple points (yellow arrowheads in Figures 2A and 2A′). At the 2S stage (Figure 2B), however, the junctions were located at lateral positions, leaving adjacent cells separated by a narrow, slit-like extracellular space (asterisks in Figure 2B′). At the 3–5S stage (Figure 2C), this extracellular space was increased, forming a vascular lumen larger than 5 μm, the diameter of capillaries, the smallest functional blood vessels in vertebrates. We refer to dorsal aortae with a lumen smaller than 5 μm in diameter as "cords" (Figures 2A and 2B), and dorsal aortae with a lumen larger than 5 μm as "tubes" (Figures 2C and 2D). At the 6–8S stage (Figure 2D), the aortic lumen was larger than 20 μm in diameter and the ECs were significantly thinner compared to the 1–2S stage. We conclude that initiation of lumen formation in the dorsal aortae is accompanied by relocalization of junctions, formation and increase of extracellular space between adjacent ECs, and cell shape changes.

Experiments in zebrafish embryos led to the proposal that vascular lumen formation is driven by the production of large intracellular vacuoles that remain in ECs for several hours (Kamei et al., 2006). In contrast, our comprehensive EM analysis of 33 mouse embryos and 230 transverse sections through the developing dorsal aortae during the short transition from cord to tube (E8.0–E8.25) did not reveal any intracellular vacuoles with a diameter larger than 0.5 μm (Figure 2E). Although vacuole-like structures were occasionally observed in transverse sections (see small asterisk in Figure S1B), the complete series of sections through the developing dorsal aortae revealed that these structures were plasma membrane invaginations rather than intracellular vacuoles (Figures S1A and S1C–S1L).

In line with the hypothesis that targeting of exocytotic vesicles to the future luminal plasma membrane is important for creating a multicellular lumen, we observed small vesicles, constituting less than 1% of the luminal area, within ECs during the transition from cord to a vascular tube (Figures 2F and 2G). Moreover, consistent with the observation that most developing blood vessels are initially permeable, we showed that the developing aortic lumen is continuous with the surrounding extravascular interstitium due to the presence of paracellular openings (arrowhead in Figure 2H).

Taken together, these data suggest that the aortic lumen develops extracellularly at the cell-cell contact between adjacent ECs.

CD34-Sialomucins, Moesin, F-Actin, and Non-Muscle Myosin II Localize to the Endothelial Cell-Cell Contact at the Onset of Aortic Lumen Formation

Formation of the apical plasma membrane is thought to be a key step during lumen formation in epithelial cells (reviewed by Bryant and Mostov, 2008; Lubarsky and Krasnow, 2003). In these cells, Podocalyxin (PODXL or gp135) is commonly used as an apical cell surface marker (Meder et al., 2005). It belongs to the family of functionally redundant CD34-sialomucins (reviewed be Nielsen and McNagny, 2008), all of which are expressed in ECs.

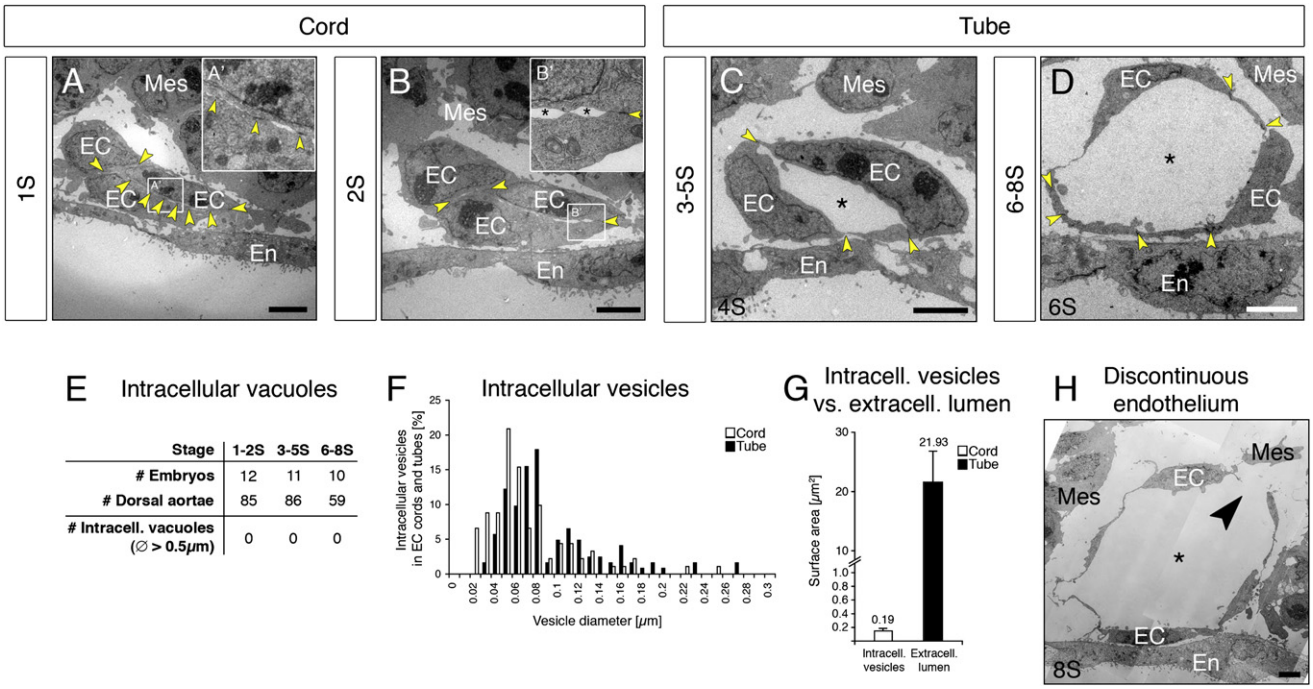

Figure 2. Extracellular Vascular Lumen Formation in the Developing Aorta

(A–D) Electron micrographs of ultrathin transverse sections through aortic endothelial cells (ECs) at the indicated stages of mouse development. En, endoderm; Mes, mesenchyme. Scale bars, 5 μm. (A) 1S stage: adjacent ECs joined by junctions (yellow arrowheads). (A′) Higher magnification of the depicted area in (A). (B) 2S stage: adjacent ECs with junctions (yellow arrowheads) at lateral positions separated by a slit-like extracellular space. (B′) Higher magnification of the depicted area in (B). (C) 3-5S stage: ECs are separated by an increased extracellular space (asterisk). (D) 6–8S stage: thin ECs surround a vascular lumen.

(E) Quantification of intracellular vacuoles larger than 0.5 μm. Numbers of embryos and aortic sections analyzed by electron microscopy (EM) are indicated.

(F) Quantification of the diameter of intracellular vesicles based on EM images of transverse sections through aortic ECs present in EC cords and vascular tubes; n = 50 dorsal aortae present as either cord or tube of n ≥ 3 embryos.

(G) Quantification of the area of intracellular vesicles in cords and the extracellular luminal area in vascular tubes based on EM images of transverse sections through aortic ECs; n = 50 dorsal aortae present as either cord or tube of n ≥ 3 embryos. Values are means ± SEM.

(H) Electron micrograph of an ultrathin transverse section through the developing aorta (8S stage) shows that the vascular lumen (asterisk) is continuous with the extravascular interstitium through a paracellular opening (arrowhead). Scale bar, 5 μm.

In aortic ECs, we found two CD34-sialomucins (CD34 and PODXL) present at the early onset of vascular lumen formation (Figures 3A–3F). Immunostaining of transverse sections through the developing dorsal aortae revealed a cytoplasmic vesicular distribution of CD34 and PODXL at the 1S stage (Figures 3A and 3B). In contrast, at the 2S stage, both CD34-sialomucins were predominantly localized at the cell-cell contact of adjacent ECs, thus defining the endothelial cell-cell contact as the apical site where the future aortic lumen develops (Figures 3C and 3D). At the 3S stage and thereafter, the CD34-sialomucins preferentially localize to the luminal or apical plasma membranes (Figures 3E and 3F, and data not shown).

CD34-sialomucins are linked to the F-actin cytoskeleton via Ezrin-Radixin-Moesin (ERM) adaptor proteins (reviewed by Bretscher et al., 2002), known to be important for epithelial tubulogenesis (Gobel et al., 2004; Van Furden et al., 2004). Since the ERM protein Moesin has been shown to be particularly abundant in ECs (reviewed by Nielsen and McNagny, 2008), we asked whether Moesin and F-actin colocalize with the CD34-sialomucins at the onset of aortic lumen formation.

At the 1S stage, Moesin was mainly localized in the cytoplasm (Figure 3G) and F-actin was localized along the entire EC surface (Figure 3H). However, at the 2S stage, after the appearance of CD34-sialomucins at the endothelial cell-cell contact (Figures 3C and 3D), Moesin and F-actin were also enriched at the cell-cell contact (Figures 3I and 3J). Consistent with its role as an adaptor between CD34-sialomucins and F-actin, Moesin colocalized with both PODXL and F-actin in ECs (data not shown). Subsequently, Moesin and F-actin localized at the luminal or apical plasma membranes at the 3S stage and thereafter (Figures 3K and 3L, and data not shown). In line with the notion that only phosphorylated ERM proteins link CD34-sialomucins with F-actin (reviewed by Bretscher et al., 2002), Moesin was found to be phosphorylated at the luminal cell surface in ECs throughout vascular lumen formation (Figures S2A, S2D, and S2G).

F-actin is known to interact with non-muscle (nm) Myosin II to induce cell shape change in different cell types, including ECs (Furman et al., 2007). At the 1S stage, nm-Myosin II was evenly distributed within the cell (Figure 3M), but during the transition from the 2S to the 3S stage, it became enriched at the endothelial cell-cell contact and the luminal cell surface (Figures 3N and 3O). At the same time, the ECs elongated and formed a vascular lumen (Figures 3P–3R and Figures S3A–S3I).

These data show that CD34-sialomucins, Moesin, and F-actin localize to the endothelial cell-cell contact, thus forming the apical pole of vascular lumen formation. In addition, the data

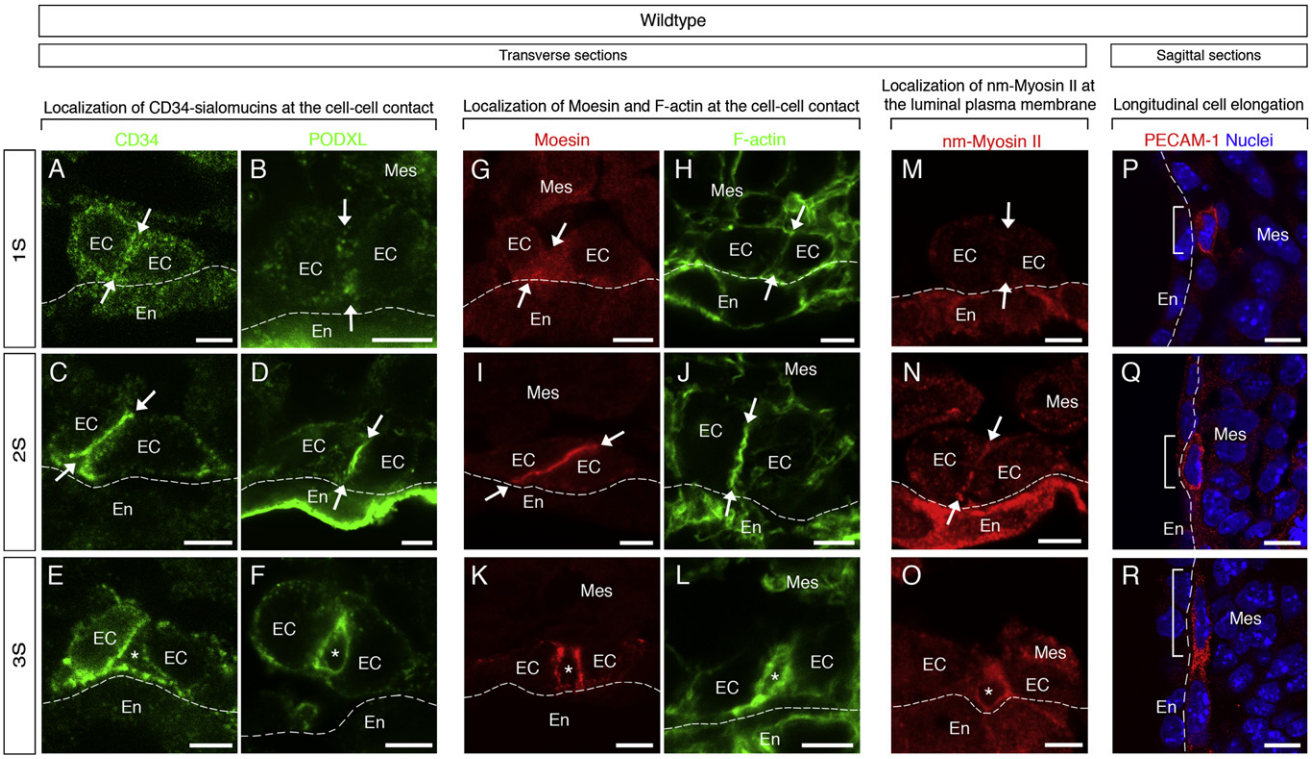

Figure 3. Localization of CD34-Sialomucins, Moesin, F-Actin, and nm-Myosin II at the Endothelial Cell-Cell Contact at the Onset of Vascular Lumen Formation

Confocal images of (A–O) transverse and (P–R) sagittal sections through the developing dorsal aortae. Arrows point to the endothelial cell-cell contact. Asterisks mark the developing lumen. En, endoderm; Mes, mesenchyme. 1S: cytoplasmic staining of (A) CD34, (B) Podocalyxin (PODXL), and (G) Moesin. (H) Weak F-actin and (M) absent nm-Myosin II staining at the endothelial cell-cell contact. (P) Slightly oval-shaped EC. 2S: (C) CD34, (D) PODXL, (I) Moesin, (J) F-actin, and (N) some nm-Myosin II localize at the endothelial cell-cell contact. (Q) Slightly oval-shaped EC. 3S: (E) CD34, (F) PODXL, (K) Moesin, (L) F-actin, and (O) nm-Myosin II are enriched at the plasma membranes facing the developing vascular lumen (asterisks). (R) ECs are elongated. Scale bars, 5 μm (A–O) and 10 μm (P–R).

suggest that interaction of nm-Myosin II with apically enriched F-actin initiates the EC shape changes involved in vascular lumen formation (Figures S4A and S4B).

Vascular Endothelial-Cadherin Is Required for Localizing CD34-Sialomucins at the Endothelial Cell-Cell Contact

Since EC polarization and vascular lumen formation was observed once ECs had established a cell-cell contact, we investigated the role of the EC-specific vascular endothelial (VE)-cadherin in vascular lumen formation. Cadherins, a superfamily of calcium-dependent cell adhesion molecules, induce cell polarity in epithelial cells (Nejsum and Nelson, 2007). Therefore, we asked whether VE-Cadherin is also required for establishing cell polarity in ECs of the developing dorsal aortae.

At the 1S stage, no significant differences were observed in the dorsal aortae between control embryos and VE-Cadherin-deficient embryos (VE-Cadherin$^{-/-}$; compare upper panels of Figure 4 with upper panels of Figure 3). However, at the 3S stage, CD34, PODXL, and Moesin were not enriched at the cell-cell contact in VE-Cadherin-deficient ECs (compare Figures 3E, 3F, and 3K with Figures 4C, 4D, and 4H). In addition, as previously described (Carmeliet et al., 1999), VE-Cadherin-deficient ECs failed to form a proper vascular lumen (Figures S3J–S3R).

Phospho-Moesin was also not enriched at the endothelial cell-cell contact, but was more randomly located along the EC surface (compare Figures S2A, S2D, and S2G with Figures S2B, S2E, and S2H). Concordantly, in contrast to control embryos, in VE-Cadherin-deficient embryos, F-actin was weak and patchy at the endothelial cell-cell contact (compare Figures 3L and 4I), nm-Myosin II was absent from the apical or luminal cell surface (compare Figures 3O and 4J), and ECs did not elongate (compare Figures 3R and 4L).

The defects observed in early vascular lumen formation in VE-Cadherin-deficient embryos were not due to a reduced number of ECs or an increased rate of apoptosis (Figure S5). However, in agreement with previous findings (Carmeliet et al., 1999), at much later stages of development (14S), apoptotic cells were observed (Figure S5). Our data, therefore, show that apoptosis is not responsible for the alterations observed in VE-Cadherin-deficient embryos at the 1–3S stage.

In the developing dorsal aortae, VE-Cadherin flanked the PODXL-positive apical or luminal cell surface throughout the initial steps of vascular lumen formation (Figure S6). Interestingly, E-cadherin associates with the Phosphatase and Tensin homolog (PTEN) (Li et al., 2007; Vogelmann et al., 2005), which is necessary and sufficient for establishing apical cell polarity and lumen formation in MDCK epithelial cells (Martin-Belmonte

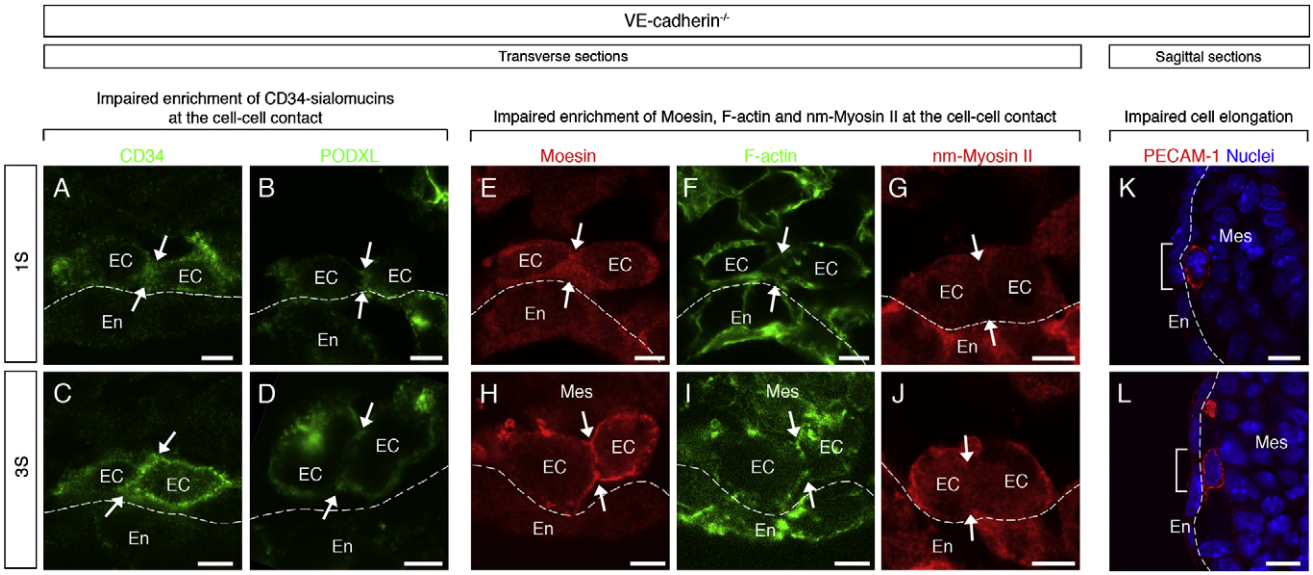

Figure 4. Impaired EC Polarization in VE-Cadherin-Deficient Mouse Embryos

Confocal images of (A–J) transverse and (K, L) sagittal sections through dorsal aortae in VE-Cadherin-deficient mouse embryos. Arrows point to the endothelial cell-cell contact. En, endoderm; Mes, mesenchyme. 1S: cytoplasmic staining of (A) CD34, (B) Podocalyxin (PODXL), and (E) Moesin. (F) Weak F-actin and (G) absent nm-Myosin II staining at the endothelial cell-cell contact. (K) Slightly oval-shaped EC. 3S: no enrichment of (C) CD34, (D) PODXL, (H) Moesin, (I) F-actin, or (J) nm-Myosin II at the endothelial cell-cell contact. (L) No EC elongation. No difference was observed between the 2S and 3S stages. Scale bars, 5 μm (A–J) and 10 μm (K, L).

et al., 2007). To test whether PTEN plays a similar role in ECs, we injected PTEN inhibitor bpV(pic) into the mesenchyme of mouse embryos at the 1S stage, and subsequently allowed these embryos to develop in whole embryo culture (WEC). WEC proved useful for studying early vascular development, since 1–2S stage embryos with no lumenized blood vessels and no heart (Figures 1A–1C) develop a functional circulatory system, fully lumenized dorsal aortae, and a beating heart in WEC (Figure S7 and data not shown). In addition, the dorsal aortae in WEC mouse embryos developed spatially and temporally similarly to mouse embryos in utero (Figure S7). Injection of bpV(pic) partially phenocopied the VE-Cadherin deficiency (Figure S8), since PODXL and Moesin were not enriched at the endothelial cell-cell contact (compare Figures S8A and S8B with Figures 4D and 4H), and a vascular lumen did not develop (Figures S8C and S8D).

Taken together, these data show that VE-Cadherin, possibly via PTEN, is required for establishing cell polarity in aortic ECs (compare Figures S4B and S4C).

PODXL and Moesin Are Required for Early Vascular Lumen Formation

Since VE-Cadherin was required for PODXL and Moesin localization at the endothelial cell-cell contact, we asked whether these proteins are also functionally involved in aortic lumen formation (Figure S9). We first analyzed mice deficient for PODXL (Doyonnas et al., 2001) at the 3S stage, when a small lumen has started to develop. Importantly, in the absence of PODXL, Moesin was diffusively distributed in the cytoplasm (compare Figures S9D and S9E), and F-actin was distributed along the entire plasma membranes rather than enriched at the endothelial cell-cell contact (compare Figures S9G and S9H). In addition, at the 6–8S stage, 40% of the PODXL-deficient dorsal aortae had not yet formed a vascular tube, while the control dorsal aortae had fully lumenized (Figure S9M, compare Control with PODXL$^{-/-}$). Finally, the diameter of the aortic lumen in PODXL-deficient embryos was less than half that of the control diameter (compare Figures S9J and S9K, and Figure S9N).

We next analyzed mice deficient for Moesin (Moesin$^{-/-}$) (Doi et al., 1999), and observed that PODXL was correctly positioned at the endothelial cell-cell contact (Figure S9C). However, consistent with its role as an adaptor between CD34-sialomucins and F-actin, the F-actin was not enriched at the cell-cell contact where PODXL was found (compare Figures S9G and S9I). Finally, at the 6–8S stage, 20% of the Moesin-deficient dorsal aortae had not formed a vascular tube (Figure S9M, compare Control with Moesin$^{-/-}$), and the diameter of the aortic lumen was about half that of the control (compare Figures S9J and S9L, and Figure S9N).

These data provide genetic evidence that PODXL and Moesin play a role in recruiting F-actin to the apical EC surface and are required for timely vascular lumen formation in the early dorsal aortae.

Protein Kinase C Activity Is Required for Moesin Phosphorylation

Only phosphorylated ERM proteins link CD34-sialomucins to the F-actin cytoskeleton (for review see Bretscher et al. [2002]). ERM protein phosphorylation is thought to involve the serine/threonine protein kinase activities of either protein kinase C (PKC) or Rho-associated protein kinase (ROCK) (Hebert et al., 2008; Ng et al., 2001). Moreover, ROCK phosphorylates and

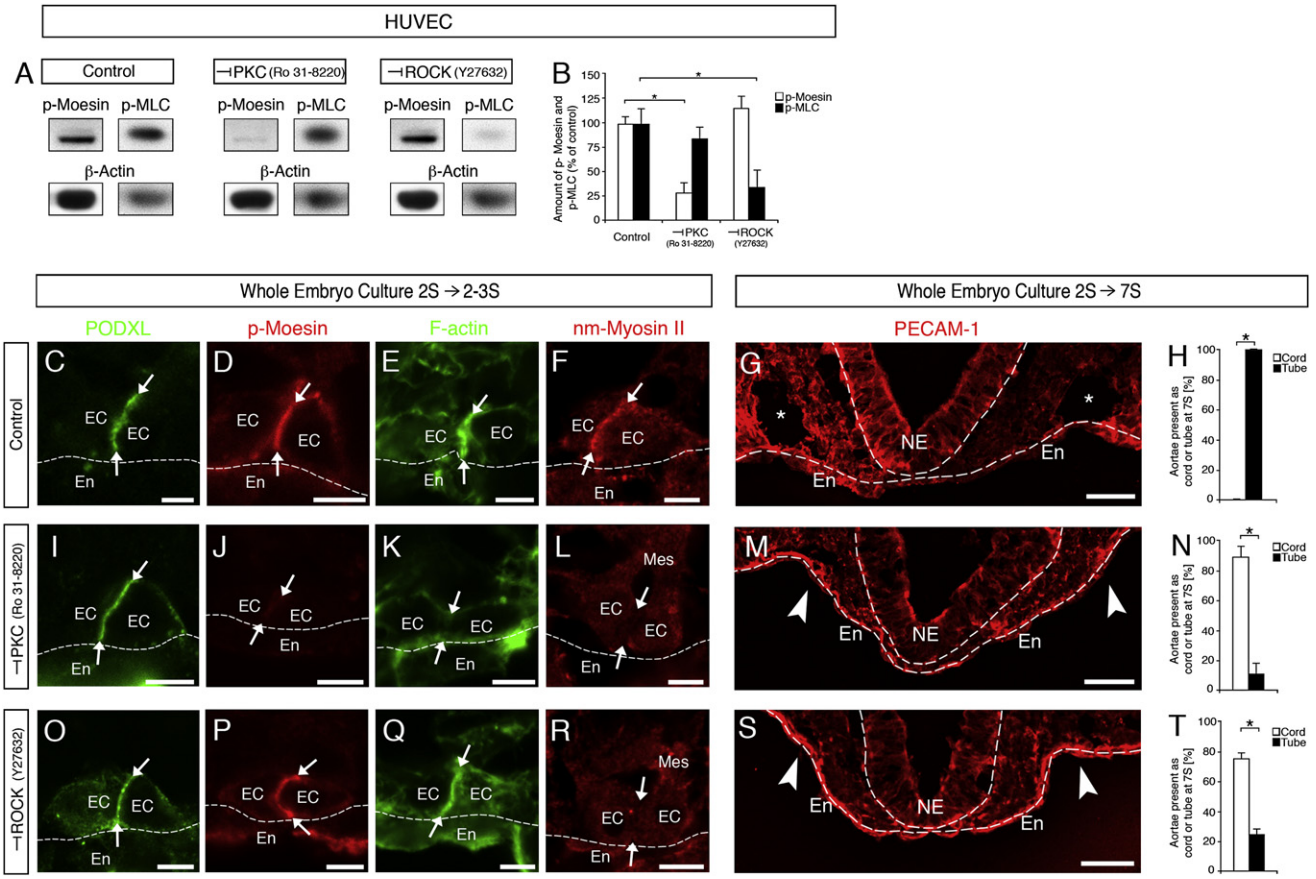

Figure 5. Protein Kinase C and Rho-Associated Protein Kinase Have Different Roles in Aortic Lumen Formation

(A and B) Different effects of protein kinase C (PKC) inhibitor Ro 31-8220 and Rho-associated protein kinase (ROCK) inhibitor Y27632 on Moesin and Myosin light chain (MLC) phosphorylation in human umbilical vein ECs (HUVECs). (A) Western blot of phospho (p)-Moesin and phospho (p)-MLC in HUVECs. (B) Quantification of the relative p-Moesin (white bars) and p-MLC levels (black bars) after inhibiting PKC (Ro 31-8220) or ROCK (Y27632). Equal amounts of cells were used, and phosphoproteins were normalized to β-actin (n = 3 experiments; *p < 0.001). All values are means ± SD.

(C–T) Effect of PKC and ROCK inhibitors on Podocalyxin (PODXL) localization, Moesin phosphorylation, F-actin and nm-Myosin II recruitment to the endothelial cell-cell contact, and formation of an aortic lumen (asterisk) in ex vivo-cultured mouse embryos. (C–F, I–L, O–R) Confocal images of transverse sections through dorsal aortae after whole-embryo culture (WEC) from the 2S to 2–3S stage for 30 min. (G, M, S) Confocal images of transverse sections through dorsal aortae after WEC from the 2S to 7S stage for 5–7 hr. Embryos were injected with (C–H) PBS, (I–N) PKC inhibitor (Ro 31-8220), or (O–T) ROCK inhibitor (Y27632). Sections were stained for the indicated markers, and arrows point to the endothelial cell-cell contact. En, endoderm; NE, neuroepithelium. Scale bars, 5 μm (C–F, I–L, O–R) and 50 μm (G, M, S). (H, N, T) Quantification of cords and tubes after WEC from the 2S to 7S stage after the treatment indicated on the left (n ≥ 100 [control] or n ≥ 200 aortic sections [treatment] of n ≥ 3 embryos per condition; *p < 0.05). All values are means ± SD.

activates Myosin regulatory light chain (MLC), which is generally required for actomyosin-based cell shape changes (reviewed by Riento and Ridley, 2003). We therefore investigated whether the kinase activities of PKC and ROCK are required for phosphorylation of Moesin and MLC in human umbilical vein ECs (HUVECs).

We used Ro 31-8220 as a pan-PKC inhibitor to inhibit the PKC isoforms identified in sorted aortic ECs (Figure S10), and Y27632 as an inhibitor of ROCK I and II. We found that inhibition of PKC prevented phosphorylation of Moesin, but did not affect phosphorylation of MLC (Figures 5A and 5B, compare PKC inhibitor with Control). Conversely, inhibition of ROCK prevented phosphorylation of MLC, but did not affect Moesin phosphorylation (Figures 5A and 5B, compare ROCK inhibitor with Control). These specific effects of PKC on Moesin phosphorylation and of ROCK on MLC phosphorylation were also confirmed with a different set of inhibitors (Figure S11).

In order to further confirm these findings in the developing mouse dorsal aortae, and to investigate whether PKC and ROCK affect aortic lumen formation, we analyzed mouse embryos injected with the respective inhibitors (Figures 5C–5T). When the PKC inhibitor Ro 31-8220 was injected, PODXL correctly localized to the endothelial cell-cell contact (compare Figures 5C and 5I), but Moesin failed to be phosphorylated in the aortic ECs (compare Figures 5D and 5J). Concomitantly, F-actin and nm-Myosin II were not recruited to the endothelial cell-cell contact (compare Figures 5E and 5F with Figures 5K and 5L), and ECs failed to form vascular tubes (compare Figures 5G and 5H with Figures 5M and 5N).

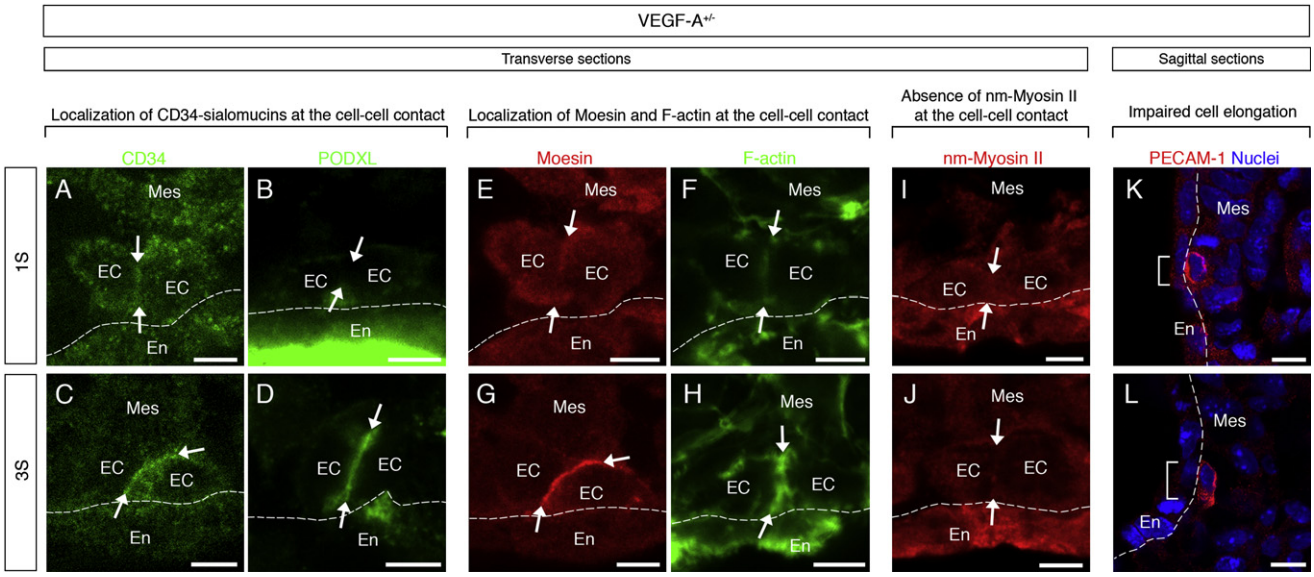

Figure 6. Impaired Recruitment of nm-Myosin II to the Endothelial Cell-Cell Contact and Lack of EC Elongation in Vascular Endothelial Growth Factor Haploinsufficient Mouse Embryos

(A–L) Confocal images of (A–J) transverse and (K, L) sagittal sections through developing dorsal aortae of vascular endothelial growth factor (VEGF)-A haploinsufficient mouse embryos. Arrows point to the endothelial cell-cell contact. En, endoderm; Mes, mesenchyme. 1S: cytoplasmic staining of (A) CD34, (B) Podocalyxin (PODXL), and (E) Moesin. (F) Weak F-actin and (I) absent nm-Myosin II staining at the endothelial cell-cell contact. (K) Slightly oval-shaped EC. 3S: (C) CD34, (D) PODXL, (G) Moesin, and (H) F-actin, but not (J) nm-Myosin II, localize at the endothelial cell-cell contact. (L) No EC elongation. No difference was observed between the 2S and 3S stages. Scale bars, 5 μm (A–J) and 10 μm (K, L).

When the ROCK-inhibitor Y27632 was injected, PODXL localized to the endothelial cell-cell contact (compare Figures 5C and 5O), Moesin phosphorylation was not inhibited (compare Figures 5D and 5P), and F-actin was appropriately recruited to the endothelial cell-cell contact (compare Figures 5E and 5Q). However, nm-Myosin II, which requires MLC phosphorylation for its interaction with F-actin (reviewed by Riento and Ridley, 2003), failed to localize to the F-actin at the endothelial cell-cell contact (compare Figures 5F and 5R), and the ECs formed vascular tubes to a lesser extent (compare Figures 5G and 5H with Figures 5S and 5T).

PKC activity is therefore required for Moesin phosphorylation and F-actin recruitment to the endothelial cell-cell contact, whereas ROCK activity is required for MLC phosphorylation and nm-Myosin II recruitment to the apically enriched F-actin.

Vascular Endothelial Growth Factor-A Activates ROCK and MLC, Enabling nm-Myosin II Recruitment to the Endothelial Cell-Cell Contact and EC Shape Change

Vascular endothelial growth factor (VEGF)-A regulates ROCK activity (Nacak et al., 2007; Sun et al., 2006), and is required for embryonic blood vessel formation (Carmeliet et al., 1996; Ferrara et al., 1996). To investigate the role of VEGF-A in aortic lumen formation, we crossed PGK-Cre mice, expressing Cre recombinase early and ubiquitously (Lallemand et al., 1998) with VEGF-A*loxP* mice (Gerber et al., 1999) to obtain haploinsufficient VEGF-A$^{+/-}$ mouse embryos (Figure 6). These embryos completely failed to form lumenized dorsal aortae (Figures S3S–S3AA) despite the surprisingly normal polarization of the aortic ECs (i.e., CD34, PODXL, Moesin, and F-actin were recruited to the endothelial cell-cell contact [Figures 6C, 6D, 6G, and 6H]). Moesin was also normally phosphorylated (Figures S2C, S2F, and S2I). Nm-Myosin II, however, was completely absent from the endothelial cell-cell contact (Figure 6J), and the ECs did not elongate in VEGF-A haploinsufficient mouse embryos (Figures 6K and 6L). Importantly, these early defects in aortic lumen formation were not attributable to either a reduced EC number or an increased apoptosis rate (Figure S5).

Because both VEGF-A and ROCK were found to be required for the recruitment of nm-Myosin II to the apical cell surface at the endothelial cell-cell contact, we asked whether VEGF-A is upstream of ROCK (Figures S12A–S12D). Accordingly, we stimulated HUVECs with VEGF-A, and analyzed the activity of ROCK and its downstream signal MLC. Our data show that VEGF-A significantly increased ROCK activity (Figures S12A and S12B) and activated MLC, as measured by MLC phosphorylation (Figures S12C and S12D). Moreover, VEGF-A signaling was required for MLC activation, as application of the VEGF-A signaling inhibitors, Flt1-Fc and SU5416, significantly decreased MLC phosphorylation in HUVECs (Figures S12C and S12D).

We next inhibited VEGF-A signaling in WEC using these two pharmacological inhibitors (Figures S12E–S12S). Importantly, the VEGF-A signaling inhibitors reproduced the effects observed in VEGF-A haploinsufficient (VEGF-A$^{+/-}$) mouse embryos (Figures S12E–S12S). In particular, when SU5416 was used at a concentration 40× higher than that to fully block VEGF receptor signaling in HUVECs (Mendel et al., 2000), EC polarity was properly established (i.e., both PODXL and Moesin were enriched at the endothelial cell-cell contact, and Moesin was phosphorylated [Figures S12O and S12P]). In contrast, nm-Myosin II was not recruited to the apical cell surface (compare Figures S12G and S12Q), and the ECs did not form vascular tubes (compare

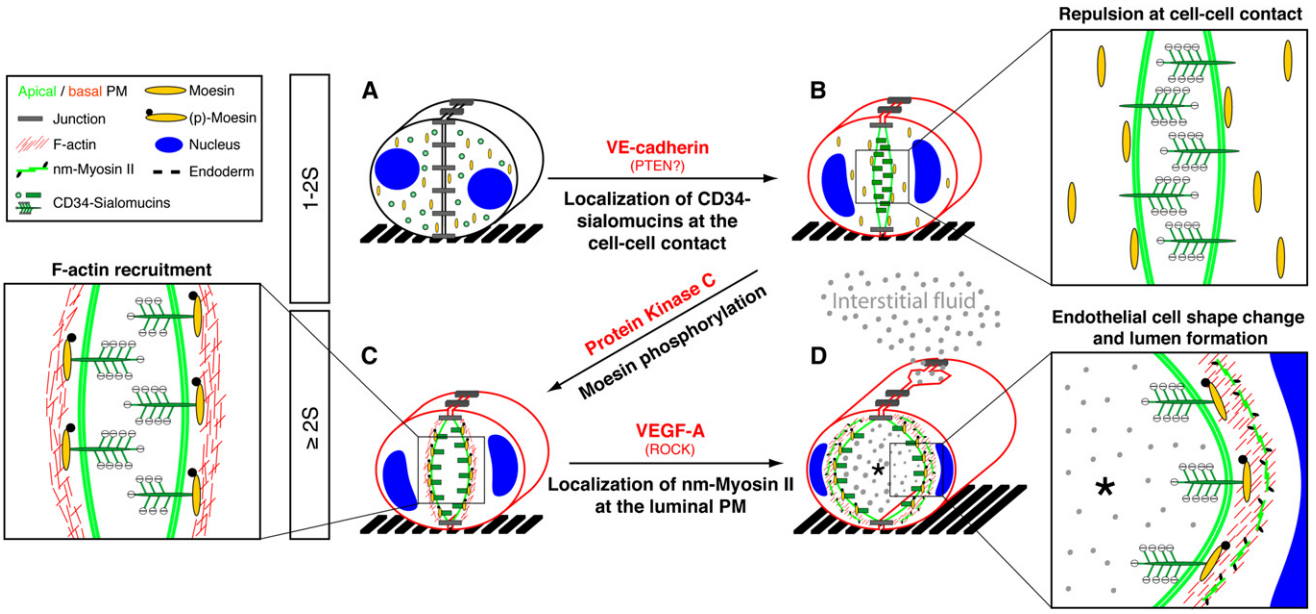

Figure 7. Molecular Mechanism of In Vivo Vascular Lumen Formation in the Developing Aorta

(A) Adjacent ECs adhere to each other via junctions at multiple positions along the endothelial cell-cell contact.

(B) VE-Cadherin is required for localizing of CD34-sialomucins to the endothelial cell-cell contact, possibly via its interaction with Phosphatase and Tensin homolog. The antiadhesive CD34-sialomucins are involved in separating apical EC surfaces from each other.

(C) PKC activity is required for phosphorylating Moesin, which is involved in recruiting F-actin to the apical cell surface at the endothelial cell-cell contact.

(D) VEGF-A activates ROCK, which is required for MLC phosphorylation and recruitment of nm-Myosin II to the apically enriched F-actin. VEGF-A and ROCK are required for fully separating apical EC surfaces from each other, for EC shape changes, and for vascular lumen formation. In in vitro vascular tubes, the F-actin is oriented parallel to the longitudinal axis of the vascular lumen (data not shown), suggesting a similar F-actin orientation in the developing aorta. Since the developing lumen (asterisk) is leaky, extravascular interstitial fluid (gray dots) passively enters via paracellular openings.

Figures S12H and S12I with Figures S12R and S12S). The only lumenized dorsal aortae were observed cranially and caudally, far away from the injection sites (data not shown).

Combined, our data strongly suggest that VEGF-A signaling is not required for EC polarization and Moesin phosphorylation, but is specifically required for recruitment of nm-Myosin II to the endothelial cell-cell contact, EC shape change, and aortic lumen formation (compare Figures S4B and S4D).

DISCUSSION

The circulatory system is the first functional organ system to develop in vertebrates. Its proper function strictly depends on lumenized blood vessels to execute vital tasks, such as the transport of blood cells, nutrients, gases, and wastes to and from all organs and tissues. During blood vessel formation, ECs are the only cell type capable of forming lumenized vascular tubes. The first study on in vivo vascular lumen formation in zebrafish suggested that large intracellular vacuoles developed in ECs and remained there for several hours before coalescing with the vacuoles from adjacent ECs (Kamei et al., 2006). However, recently, another study on the same blood vessels in zebrafish suggested that the vascular lumen did not develop via vacuole coalescence, but instead developed extracellularly between adjacent ECs (Blum et al., 2008). Neither study suggested a molecular mechanism of vascular lumen formation, or explained the role of key factors, such as VE-Cadherin or VEGF-A, in their particular models.

Formation of an Apical Cell Surface at the Endothelial Cell-Cell Contact

Here, we performed a detailed structure/function analysis of the developing aorta to propose a molecular mechanism of in vivo vascular lumen formation (Figure 7; Movie S2). Interestingly, similar to lumen formation in blood vessels of other systems (Blum et al., 2008; Jin et al., 2005; Kamei et al., 2006), we observed in the developing mouse dorsal aortae that ECs first assemble in the form of an EC cord (Figure 7A) before developing a central vascular lumen. The first step in lumen formation is thus the adhesion of ECs to each other (Figure 7A). After junctional relocalization, an apical pole interface develops between adjacent ECs (Figure 7B, green color) flanked by VE-Cadherin-expressing junctions (Figure 7B, gray rectangles). The vascular lumen thus develops at the cell-cell contact between adjacent ECs (Figure 7B).

VE-Cadherin is required to form these apical cell surfaces at the endothelial cell-cell contact (Figure 7B, green color). Since we found that the apical glycoproteins, CD34 and PODXL, are located in vesicles (Figure 7A, green circles), and that PTEN is required for EC polarization, it is possible that VE-Cadherin facilitates exocytosis of apical glycoproteins at the endothelial cell-cell contact via an interaction with PTEN.

Role of CD34-Sialomucins at the Luminal Cell Surface of ECs

Once CD34-sialomucins cover the apical cell surface (Figure 7B, green rectangles), ECs de-adhere from each other and give rise

to a small slit at the endothelial cell-cell contact (Figure 7B, green color). Interestingly, cell-cell repulsion as a mechanism of lumen formation has been recently described for heart formation in *Drosophila* (Medioni et al., 2008; Santiago-Martinez et al., 2008), and the apical cell surface glycoproteins, CD34 and PODXL, have been shown to be antiadhesive due to their negatively charged glycosyl residues (reviewed by Nielsen and McNagny, 2008). Importantly, deletion of PODXL was sufficient to significantly delay aortic lumen formation in mouse embryos, showing that apical antiadhesive glycoproteins play a functional role in generating an extracellular vascular lumen at the endothelial cell-cell contact (Figure 7B, green rectangles).

Recruitment of F-Actin to the Luminal Cell Surface

CD34-sialomucins connect with the F-actin cytoskeleton via functionally redundant ERM proteins (reviewed by Bretscher et al. [2002]). Moesin appears to be the most abundant ERM protein in mammalian ECs (Koss et al., 2006; Okada et al., 2005) (yellow ovals in Figures 7B and 7C), and we found that deletion of Moesin in mice delays aortic lumen formation and decreases the amount of apical F-actin in early aortic ECs. In addition, loss of PODXL reduces the amount of Moesin and F-actin located at the endothelial cell-cell contact, suggesting that PODXL connects with Moesin in order to recruit F-actin and facilitate vascular lumen formation (Figures 7B–7C).

Moesin must be phosphorylated in order to link CD34-sialomucins with the F-actin cytoskeleton (reviewed by Bretscher et al. [2002]). Here, we show that PKC, but not ROCK, is required for Moesin phosphorylation in aortic ECs (Figures 7B–7C). Interestingly, aortic ECs express several novel PKC (nPKC) and atypical PKC (aPKC) isoforms during aortic lumen formation, and microarrays of HUVECs, cultured in monolayers and lumenized sprouts, showed that nPKC-theta, along with nPKC-eta, is upregulated upon in vitro vascular lumen formation (data not shown). Thus, a PKC-dependent step leads to the phosphorylation of Moesin (Figures 7B–7C), which directly or indirectly links the F-actin cytoskeleton (Figure 7C, red lines) to the apical CD34-sialomucins in aortic ECs.

VEGF-A-Dependent EC Shape Change

We show that VEGF-A increases ROCK activity (Figures 7C and 7D), and that this is required for activating MLC and recruiting nm-Myosin II (Figure 7D, green bars) to the apical EC surface. These observations suggest that VEGF-A induces the formation of an actomyosin complex at the apical cell surface to promote endothelial cell-cell separation, leading to vascular lumen formation (Figures 7C and 7D). Since the developing vascular lumen is leaky, interstitial fluid should be able to passively enter the lumen via paracellular openings (Figure 7D, gray dots).

A Molecular Model for In Vivo Vascular Lumen Formation

Our study on the developing aorta has yielded a molecular mechanism by which a vascular lumen forms in vivo (Figure 7, Movie S2). In addition, localization of CD34, PODXL, and Moesin at the endothelial cell-cell contact was also found during blood vessel formation in the developing lung and kidney, as well as in Lewis lung carcinoma (Figure S13). It is thus likely that many aspects of the proposed molecular mechanism are applicable to vascular lumen formation in other developing blood vessels.

EXPERIMENTAL PROCEDURES

Mouse Strains

NMRI or C57BL/6 mice (Harlan Laboratories, Horst, The Netherlands) were used for wild-type studies and WEC. PODXL$^{-/-}$ (Doyonnas et al., 2001), Moesin$^{-/-}$ (Doi et al., 1999), VE-Cadherin$^{-/-}$ (Carmeliet et al., 1999), VEGF-A*loxP* (Gerber et al., 1999), and PGK-Cre mice (Lallemand et al., 1998) have previously been described. Littermates or mouse embryos of similar genetic background were used as controls.

Mouse Embryo Isolation

Isolated mouse embryos were sorted by number of somites. After isolation or WEC, all embryos were fixed in either 4% paraformaldehyde (PFA) in PBS, 2.5% glutaraldehyde with 2% PFA in 0.1 M Na-cacodylate buffer, or 5% trichloroacetic acid in PBS, and further processed for imaging.

Embryonic Injections and Whole-Embryo Culture

All embryos were isolated, dissected, and kept in PBS (+Mg^{2+}, +Ca^{2+}) at 37°C during injection. For WEC, all substances were injected in an aqueous solution containing phenol red diluted 1:10 in PBS in order to monitor their localization. 200 μM Ro 31-8220 (Biaffin), 200 μM Y27632 (Calbiochem), 500 ng/ml Flt1-Fc (R&D Systems), 200 μM SU5416 (Sigma), or 200 μM bpV(pic) (Merck Biosciences) was injected into embryos at the 1S or 2S stage from the ventral side through the endoderm into the mesenchyme. PBS alone, 1% DMSO, or 500 ng/ml IgG_1-Fc (R&D Systems) served as controls. After injection, embryos were transferred into rat serum (Charles River Laboratories) containing 1% HEPES, and were roller-cultured (WEC) at 37°C with 5% O_2 for the indicated times. After WEC, embryos were processed for immunostaining and imaging.

Immunostaining and Imaging

For confocal light microscopy, fixed embryos were cryopreserved in 30% sucrose (Sigma), embedded in OCT (Fisher Scientific), and cryosectioned at 12 μm for transverse and 40 μm for sagittal sections, or kept intact for whole-mount staining for SPIM. The following antibodies were used: rabbit anti-Caspase3 (active) (Sigma), rat anti-CD34 (eBioscience), rabbit anti-Moesin (Abcam), rabbit anti-nm-Myosin II heavy chain A (Covance Research), rabbit anti-phospho-Moesin (Santa Cruz Biotechnology), rat anti-PECAM-1 (BD Bioscience), goat anti-PODXL (R&D Systems), and rat anti-VE-Cadherin (Millipore). DAPI (Sigma) was used to stain cell nuclei, and Alexa Fluor (AF) 488-conjugated phalloidin (Molecular Probes) to stain F-actin. Secondary antibodies were conjugated with AF488 or AF633 (Molecular Probes) and Cy3 or Cy5 (Jackson ImmunoResearch). Images were acquired and analyzed using a Zeiss 510 LSM or a Zeiss SPIM prototype. For the analysis of aortic lumens in mouse embryos, transverse sections through the entire embryo were analyzed. Projections and movies were generated using LSM 510 software (Zeiss) or ImageJ (NIH), respectively. To identify ECs, all sections were co-stained with either PECAM-1 or CD34. Preparation of samples for EM was described previously (Kucera et al., 2009).

In Vitro Studies

HUVECs (Lonza) of passages < P8 were used for all experiments. Cells were grown in EGM2 medium (Lonza) and incubated at 37°C and 5% CO_2. For inhibition studies of PKC and ROCK, HUVECs were grown to confluence and incubated with EGM2 containing 5 μM Ro 31-8220 (Biaffin), 5 μM Y27632 (Calbiochem), 1 μM Gö6983 (Merck Biosciences), or 1 μM H-1152 (Merck Biosciences) for 30 min. For studies addressing activation by VEGF-A or inhibition of VEGF-A signaling, HUVECs were grown to 90% confluence and starved for 6 hr in starvation medium (EGM2 + 0.5% FCS). Subsequently, cells were incubated with starvation medium alone or supplemented with 2.5 μg/ml Flt1-Fc or 5 μM SU5416 for 30 min, followed by stimulation with 10 ng/ml VEGF-A165 (Biomol) for 10 min alone or with 2.5 μg/ml Flt1-Fc or 5 μM SU5416. For the measurement of ROCK activity (Cell Biolabs, Inc.), cells were starved for 6 hr and subsequently stimulated with 10 ng/ml VEGF-A165 for 10 min. Starvation medium alone, 1% DMSO, or 2.5 μg/ml IgG_1-Fc served as controls. For immunoblotting, rabbit anti-phospho-MLC (Cell Signaling), rabbit anti-phospho-Moesin (Abcam), and mouse anti-β-actin (Sigma) antibodies were used in combination with HRP-conjugated secondary antibodies (Dianova). Equal amounts of cells were used, and phosphoproteins were

normalized to β-actin for each experiment. Band intensity was quantified using ImageJ (NIH).

PKC Expression Analysis in Aortic ECs

Embryos (1-6S) were isolated, freed from the yolk sac, cardiogenic plate, and amnion, and incubated in dissociation solution (2.5 mg/ml collagenase IV, 10 mg/ml dispase II, 0.12 mg/ml DNase in HBSS) for 2 hr at 37°C with slow agitation. Cell suspensions were incubated with anti-PECAM-1 primary antibody (BD Bioscience) and AF488-conjugated secondary antibody (Molecular Probes), FAC sorted for PECAM-1-positive ECs (i.e, dorsal aorta) and PECAM-1-negative cells (i.e., embryo), followed by cDNA synthesis and PCR (for a list of primers, see Table S1). A mixture of tissues from an adult mouse served as a positive control.

Statistical Analysis

Data are presented as means ± SD or ± SEM (see figure legends). Student's t tests were used for statistical analysis; $p < 0.05$ was considered statistically significant.

SUPPLEMENTAL DATA

Supplemental Data include thirteen figures, one table, and two movies and can be found with this article online at http://www.cell.com/developmental-cell/supplemental/S1534-5807(09)00349-9/.

ACKNOWLEDGMENTS

We thank our friends and colleagues for helpful discussions, and are grateful to B. Wielockx for tumor samples and to S. Preibisch and P. Tomancak for three-dimensional visualization of the SPIM images. We also thank W. Huttner, G. Ehninger, M. Zerial, G. Breier, K. Simons, C. Thiele, L. Rohde, I. Nüsslein, and U. Rüther for their kind support. We also thank B. Radt and H. Lippert (Zeiss) for working with us on the SPIM image acquisition. The project was funded by the Deutsche Forschungsgemeinschaft (SFB655 "Cells into Tissues"), the Behrens-Weise Foundation, and the Heinrich-Heine-University of Düsseldorf. T.K. was supported by research project MSM 0021620807 from the Ministry of Education, Youth, and Sports of the Czech Republic. B.S. and J.E. were members of the International Max Planck Research School for Molecular Cell Biology and Bioengineering. K.M.M. is a Michael Smith Foundation for Health Research Scholar, and the work of K.M.M. and M.R.H. was funded by grants from the Heart and Stroke Foundation of British Columbia and The Yukon and the Canadian Institutes for Health Research. N.F. is an employee and shareholder of Genentech, Inc.

Received: January 11, 2009
Revised: June 28, 2009
Accepted: August 26, 2009
Published: October 19, 2009

REFERENCES

Blum, Y., Belting, H.G., Ellertsdottir, E., Herwig, L., Luders, F., and Affolter, M. (2008). Complex cell rearrangements during intersegmental vessel sprouting and vessel fusion in the zebrafish embryo. Dev. Biol. *316*, 312–322.

Bretscher, A., Edwards, K., and Fehon, R.G. (2002). ERM proteins and merlin: integrators at the cell cortex. Nat. Rev. Mol. Cell Biol. *3*, 586–599.

Bryant, D.M., and Mostov, K.E. (2008). From cells to organs: building polarized tissue. Nat. Rev. Mol. Cell Biol. *9*, 887–901.

Carmeliet, P., Ferreira, V., Breier, G., Pollefeyt, S., Kieckens, L., Gertsenstein, M., Fahrig, M., Vandenhoeck, A., Harpal, K., Eberhardt, C., et al. (1996). Abnormal blood vessel development and lethality in embryos lacking a single VEGF allele. Nature *380*, 435–439.

Carmeliet, P., Lampugnani, M.G., Moons, L., Breviario, F., Compernolle, V., Bono, F., Balconi, G., Spagnuolo, R., Oostuyse, B., Dewerchin, M., et al. (1999). Targeted deficiency or cytosolic truncation of the VE-cadherin gene in mice impairs VEGF-mediated endothelial survival and angiogenesis. Cell *98*, 147–157.

Czirok, A., Zamir, E.A., Szabo, A., and Little, C.D. (2008). Multicellular sprouting during vasculogenesis. Curr. Top. Dev. Biol. *81*, 269–289.

Davis, G.E., and Camarillo, C.W. (1996). An alpha 2 beta 1 integrin-dependent pinocytic mechanism involving intracellular vacuole formation and coalescence regulates capillary lumen and tube formation in three-dimensional collagen matrix. Exp. Cell Res. *224*, 39–51.

Doi, Y., Itoh, M., Yonemura, S., Ishihara, S., Takano, H., Noda, T., and Tsukita, S. (1999). Normal development of mice and unimpaired cell adhesion/cell motility/actin-based cytoskeleton without compensatory up-regulation of ezrin or radixin in Moesin gene knockout. J. Biol. Chem. *274*, 2315–2321.

Doyonnas, R., Kershaw, D.B., Duhme, C., Merkens, H., Chelliah, S., Graf, T., and McNagny, K.M. (2001). Anuria, omphalocele, and perinatal lethality in mice lacking the CD34-related protein podocalyxin. J. Exp. Med. *194*, 13–27.

Drake, C.J., and Fleming, P.A. (2000). Vasculogenesis in the Day 6.5 to 9.5 mouse embryo. Blood *95*, 1671–1679.

Ferrara, N., Carver-Moore, K., Chen, H., Dowd, M., Lu, L., O'Shea, K.S., Powell-Braxton, L., Hillan, K.J., and Moore, M.W. (1996). Heterozygous embryonic lethality induced by targeted inactivation of the VEGF gene. Nature *380*, 439–442.

Folkman, J., and Haudenschild, C. (1980). Angiogenesis in vitro. Nature *288*, 551–556.

Furman, C., Sieminski, A.L., Kwiatkowski, A.V., Rubinson, D.A., Vasile, E., Bronson, R.T., Fassler, R., and Gertler, F.B. (2007). Ena/VASP is required for endothelial barrier function in vivo. J. Cell Biol. *179*, 761–775.

Gerber, H.P., Hillan, K.J., Ryan, A.M., Kowalski, J., Keller, G.A., Rangell, L., Wright, B.D., Radtke, F., Aguet, M., and Ferrara, N. (1999). VEGF is required for growth and survival in neonatal mice. Development *126*, 1149–1159.

Gobel, V., Barrett, P.L., Hall, D.H., and Fleming, J.T. (2004). Lumen morphogenesis in *C. elegans* requires the membrane-cytoskeleton linker ERM-1. Dev. Cell *6*, 865–873.

Hebert, M., Potin, S., Sebbagh, M., Bertoglio, J., Breard, J., and Hamelin, J. (2008). Rho-ROCK-dependent ezrin-radixin-Moesin phosphorylation regulates Fas-mediated apoptosis in Jurkat cells. J. Immunol. *181*, 5963–5973.

Jin, S.W., Beis, D., Mitchell, T., Chen, J.N., and Stainier, D.Y. (2005). Cellular and molecular analyses of vascular tube and lumen formation in zebrafish. Development *132*, 5199–5209.

Kamei, M., Saunders, W.B., Bayless, K.J., Dye, L., Davis, G.E., and Weinstein, B.M. (2006). Endothelial tubes assemble from intracellular vacuoles in vivo. Nature *442*, 453–456.

Koss, M., Pfeiffer, G.R., 2nd, Wang, Y., Thomas, S.T., Yerukhimovich, M., Gaarde, W.A., Doerschuk, C.M., and Wang, Q. (2006). Ezrin/radixin/Moesin proteins are phosphorylated by TNF-alpha and modulate permeability increases in human pulmonary microvascular endothelial cells. J. Immunol. *176*, 1218–1227.

Kucera, T., Strilic, B., Regener, K., Schubert, M., Laudet, V., and Lammert, E. (2009). Ancestral vascular lumen formation via basal cell surfaces. PLoS ONE *4*, e4132. 10.1371/journal.pone.0004132.

Lallemand, Y., Luria, V., Haffner-Krausz, R., and Lonai, P. (1998). Maternally expressed PGK-Cre transgene as a tool for early and uniform activation of the Cre site-specific recombinase. Transgenic Res. *7*, 105–112.

Lammert, E., Cleaver, O., and Melton, D. (2001). Induction of pancreatic differentiation by signals from blood vessels. Science *294*, 564–567.

Li, Z., Wang, L., Zhang, W., Fu, Y., Zhao, H., Hu, Y., Prins, B.P., and Zha, X. (2007). Restoring E-cadherin-mediated cell-cell adhesion increases PTEN protein level and stability in human breast carcinoma cells. Biochem. Biophys. Res. Commun. *363*, 165–170.

Lubarsky, B., and Krasnow, M.A. (2003). Tube morphogenesis: making and shaping biological tubes. Cell *112*, 19–28.

Martin-Belmonte, F., Gassama, A., Datta, A., Yu, W., Rescher, U., Gerke, V., and Mostov, K. (2007). PTEN-mediated apical segregation of phosphoinositides controls epithelial morphogenesis through Cdc42. Cell *128*, 383–397.

Meder, D., Shevchenko, A., Simons, K., and Fullekrug, J. (2005). Gp135/podocalyxin and NHERF-2 participate in the formation of a preapical domain during polarization of MDCK cells. J. Cell Biol. *168*, 303–313.

Medioni, C., Astier, M., Zmojdzian, M., Jagla, K., and Semeriva, M. (2008). Genetic control of cell morphogenesis during *Drosophila melanogaster* cardiac tube formation. J. Cell Biol. *182*, 249–261.

Mendel, D.B., Schreck, R.E., West, D.C., Li, G., Strawn, L.M., Tanciongco, S.S., Vasile, S., Shawver, L.K., and Cherrington, J.M. (2000). The angiogenesis inhibitor SU5416 has long-lasting effects on vascular endothelial growth factor receptor phosphorylation and function. Clin. Cancer Res. *6*, 4848–4858.

Nacak, T.G., Alajati, A., Leptien, K., Fulda, C., Weber, H., Miki, T., Czepluch, F.S., Waltenberger, J., Wieland, T., Augustin, H.G., et al. (2007). The BTB-Kelch protein KLEIP controls endothelial migration and sprouting angiogenesis. Circ. Res. *100*, 1155–1163.

Nejsum, L.N., and Nelson, W.J. (2007). A molecular mechanism directly linking E-cadherin adhesion to initiation of epithelial cell surface polarity. J. Cell Biol. *178*, 323–335.

Ng, T., Parsons, M., Hughes, W.E., Monypenny, J., Zicha, D., Gautreau, A., Arpin, M., Gschmeissner, S., Verveer, P.J., Bastiaens, P.I., et al. (2001). Ezrin is a downstream effector of trafficking PKC-integrin complexes involved in the control of cell motility. EMBO J. *20*, 2723–2741.

Nielsen, J.S., and McNagny, K.M. (2008). Novel functions of the CD34 family. J. Cell Sci. *121*, 3683–3692.

Okada, T., Lopez-Lago, M., and Giancotti, F.G. (2005). Merlin/NF-2 mediates contact inhibition of growth by suppressing recruitment of Rac to the plasma membrane. J. Cell Biol. *171*, 361–371.

Parker, L.H., Schmidt, M., Jin, S.W., Gray, A.M., Beis, D., Pham, T., Frantz, G., Palmieri, S., Hillan, K., Stainier, D.Y., et al. (2004). The endothelial-cell-derived secreted factor Egfl7 regulates vascular tube formation. Nature *428*, 754–758.

Riento, K., and Ridley, A.J. (2003). ROCKs: multifunctional kinases in cell behaviour. Nat. Rev. Mol. Cell Biol. *4*, 446–456.

Sabin, F.R. (1920). Studies on the origin of blood-vessels and of red blood-corpuscles as seen in the living blastoderm of chicks during the second day of incubation. Contrib. Embryol. *9*, 215–262.

Santiago-Martinez, E., Soplop, N.H., Patel, R., and Kramer, S.G. (2008). Repulsion by Slit and Roundabout prevents Shotgun/E-cadherin-mediated cell adhesion during *Drosophila* heart tube lumen formation. J. Cell Biol. *182*, 241–248.

Sato, Y., Watanabe, T., Saito, D., Takahashi, T., Yoshida, S., Kohyama, J., Ohata, E., Okano, H., and Takahashi, Y. (2008). Notch mediates the segmental specification of angioblasts in somites and their directed migration toward the dorsal aorta in avian embryos. Dev. Cell *14*, 890–901.

Sun, H., Breslin, J.W., Zhu, J., Yuan, S.Y., and Wu, M.H. (2006). Rho and ROCK signaling in VEGF-induced microvascular endothelial hyperpermeability. Microcirculation *13*, 237–247.

Van Furden, D., Johnson, K., Segbert, C., and Bossinger, O. (2004). The *C. elegans* ezrin-radixin-Moesin protein ERM-1 is necessary for apical junction remodelling and tubulogenesis in the intestine. Dev. Biol. *272*, 262–276.

Vogelmann, R., Nguyen-Tat, M.D., Giehl, K., Adler, G., Wedlich, D., and Menke, A. (2005). TGFbeta-induced downregulation of E-cadherin-based cell-cell adhesion depends on PI3-kinase and PTEN. J. Cell Sci. *118*, 4901–4912.